Psychiatry Research: Neuroimaging 335 (2023) 111717

Contents lists available at ScienceDirect

Psychiatry Research: Neuroimaging

journal homepage: www.elsevier.com/locate/psychresns

The shape of things to come. Mapping spatiotemporal progression of striatal morphology in Huntington disease: The IMAGE-HD study

Fiona A. Wilkes [a,*], David Jakabek [b], Mark Walterfang [c,d], Dennis Velakoulis [c,d], Govinda R. Poudel [e], Julie C. Stout [f], Phyllis Chua [g], Gary F. Egan [f], Jeffrey C.L. Looi [a,c], Nellie Georgiou-Karistianis [f]

[a] Research Centre for the Neurosciences of Ageing, Academic Unit of Psychiatry and Addiction Medicine, Australian National University Medical School, Canberra Hospital, Canberra, Australia
[b] Neuroscience Research Australia, Sydney, Australia
[c] Neuropsychiatry Unit, Royal Melbourne Hospital, Melbourne Neuropsychiatry Centre, University of Melbourne and Northwestern Mental Health, Melbourne, Australia
[d] Florey Institute of Neuroscience and Mental Health, University of Melbourne, Melbourne, Australia
[e] Mary Mackillop Institute for Health Research, Australian Catholic University, Melbourne, Australia
[f] School of Psychological Sciences and the Turner Institute of Brain and Mental Health, Monash University, Melbourne, Australia
[g] Department of Psychiatry, School of Clinical Sciences, Monash University, Monash Medical Centre, Melbourne, Australia

ARTICLE INFO

Keywords:
Striatum
Endophenotype
Biomarker
Huntington's disease

ABSTRACT

Mapping the spatiotemporal progression of neuroanatomical change in Huntington's Disease (HD) is fundamental to the development of bio-measures for prognostication. Statistical shape analysis to measure the striatum has been performed in HD, however there have been a limited number of longitudinal studies. To address these limitations, we utilised the Spherical Harmonic Point Distribution Method (SPHARM-PDM) to generate point distribution models of the striatum in individuals, and used linear mixed models to test for localised shape change over time in pre-manifest HD (pre-HD), symp-HD (symp-HD) and control individuals. Longitudinal MRI scans from the IMAGE-HD study were used (baseline, 18 and 30 months). We found significant differences in the shape of the striatum between groups. Significant group-by-time interaction was observed for the putamen bilaterally, but not for caudate. A differential rate of shape change between groups over time was observed, with more significant deflation in the symp-HD group in comparison with the pre-HD and control groups. CAG repeats were correlated with bilateral striatal shape in pre-HD and symp-HD. Robust statistical analysis of the correlates of striatal shape change in HD has confirmed the suitability of striatal morphology as a potential biomarker correlated with CAG-repeat length, and potentially, an endophenotype.

1. Introduction

In Huntington's Disease (HD), atrophy of the striatum, caused by a trinucleotide repeat expansion in the *huntingtin* gene, leads to progressive motor, psychiatric and cognitive disturbances (Vonsattel et al., 1985). Striatal volume decreases 10.8 years before predicted onset of motor symptoms (van den Bogaard et al., 2011a), with more pronounced atrophy the closer an individual is to predicted onset (van den Bogaard et al., 2011b). Mapping the spatiotemporal progression of neuroanatomical change in HD (Abeyasinghe et al., 2021; Wijeratne et al., 2021), such as in the striatum, is fundamental to developing endophenotypes (intermediate phenotypes such as cognitive, motor and behavioural changes; (Gottesman and Gould, 2003), which, in turn, may lead to development of clinically relevant bio-measures suitable for staging disease and monitoring treatment response. Based on prior work (Looi and Walterfang, 2012), we explore the role of the striatum as a specific spatiotemporal *structural basis* (Looi and Santillo, 2017) that can lead to development of endophenotypes of HD through future

Abbreviations: False Discovery Rate, (FDR); Huntington's Disease, (HD); intracranial volume, (ICV); premanifest, or pre-symp-HD, (pre-HD); Schedule of Compulsions Obsessions and Pathological Impulses, (SCOPI); Spherical Harmonic Point Distribution Method, (SPHARM-PDM); symptomatic HD, (symp-HD); Estimated years to onset of disease, (YtO).

* Corresponding author at: Academic Unit of Psychiatry & Addiction Medicine, Building 4 Level 2, Australian National University School of Medicine and Psychology, Canberra Hospital, GARRAN, 2605, Australia.
E-mail address: u4314249@anu.edu.au (F.A. Wilkes).

https://doi.org/10.1016/j.pscychresns.2023.111717
Received 8 March 2023; Received in revised form 8 September 2023; Accepted 12 September 2023
Available online 14 September 2023

correlation of neuroanatomical structure and function.

1.1. Striatal shape in HD

Morphological changes in the striatum in HD were initially observed in post-mortem studies (Vonsattel and DiFiglia, 1998; Vonsattel et al., 1985), with atrophy beginning in the dorsal medial head of the caudate and putamen, as well as early loss in the tail of the caudate (Roos et al., 1985; Kassubek et al., 2004; Douaud et al., 2006; Vonsattel and DiFiglia, 1998; Vonsattel et al., 1985). This finding has been largely confirmed using more recent imaging modalities (van den Bogaard et al., 2011b; Younes et al., 2012; Looi et al., 2012; Abeyasinghe et al., 2021). Statistical shape analysis of the striatum has been performed in pre-manifest as well as symptomatic HD (pre-HD and symp-HD, respectively) (Looi et al., 2012; Younes et al., 2012; van den Bogaard et al., 2011b): small areas of shape displacement are reported to occur in people with pre-HD 11.6y from predicted disease onset (van den Bogaard et al., 2011b), with more pronounced changes occurring in the medial caudate nucleus and putamen in those closer than 10.8y to predicted onset (van den Bogaard et al., 2011b). Using an index of degree of exposure to the toxic polyglutamine repeats (CAP-score, based on CAG repeat length and age) significant shape differences can be seen in caudate and putamen in people with pre-manifest HD with high CAP scores, and in left putamen in the mid CAP scores group (Younes et al., 2012). Explosive joint torque, a measure of the motor dysfunction in HD, was found to be lower and associated with striatal shape deflation, disease burden and striatal pathology in prodromal HD compared to healthy controls (Cruickshank et al., 2020). Furthermore, early striatal degeneration has also been linked to network spread of pathology causing degeneration and disconnection in cortico-striatal pathways (Poudel et al., 2019; Tan et al., 2022a; Tan et al., 2022b)).

1.2. Mapping spatiotemporal progression of striatal atrophy in HD: the current state of play

Multiple studies have investigated longitudinal striatal volume changes in HD. A study using linear mixed methods and data from the TRACK-HD and TRACK-On-HD studies found that CAG repeat length was strongly associated with brain volumes, particularly, basal ganglia volumes, in the progression from prodromal to manifest disease, but there was limited evidence of acceleration of volume loss with ageing (Langbehn et al., 2019). Common anatomical regions with a large effect size (>0.5) differentiating between pre-manifest and manifest HD include caudate, putamen and pallidum (Wijeratne et al., 2020). Multivariate linear mixed modelling of 63 combinations of clinical and volumetric markers in HD found that individual and combined caudate and putamen volumes differentiate CAG repeat, age groups, and detected progression of disease (Abeyasinghe et al., 2021). Wijeratne and colleagues used a non-parametric Gaussian process progression model to analyse structural MRI scans of patients with HD from the TRACK-HD and PREDICT-HD cohorts, and found that there were large (20%) and early (2 years prior to disease manifestation) differences in caudate, putamen and pallidum volumes in pre-HD compared to symp-HD, where symp-HD had smaller volumes (Wijeratne et al., 2021).

To date, a limited number of studies have investigated longitudinal striatal shape change in HD (Hong et al., 2017; Muralidharan et al., 2014; Muralidharan et al., 2016; Langbehn et al., 2019; Wijeratne et al., 2020; Ramirez-Garcia et al., 2020; Bartlett et al., 2020; Abeyasinghe et al., 2021; Wijeratne et al., 2021). Using data from the PREDICT-HD study, Muralidharan and colleagues utilised diffeomorphic trajectories to compare caudate (Muralidharan et al., 2014) and right putamen (Muralidharan et al., 2016) shapes in pre-HD, with observed contraction in the head and tail and expansion in the medial body of the caudate, and deflation of the anterior and posterior aspects of the right putamen, with again some medial inflation increasing with higher CAP scores. In these studies, the significance of local shape change was not tested, nor did the authors examine for shape change association with CAG repeats. Hong and colleagues (Hong et al., 2017) have tried to address some of these issues in a feasibility study using geodesic regression from a 4D shape atlas representing normal ageing. However, they only provide qualitative differences rather than statistical testing between groups (Hong et al., 2017). Ramirez-Garcia and colleagues (Ramirez-Garcia et al., 2020) performed longitudinal surface-based analysis on 17 people with symp-HD and 17 controls, with two scans over a 16-month period: this used the FMRIB Integrated Registration and Segmentation Tool (FIRST) software of FSL version 6.0 to identify shape-deformation pattern in a vertex-wise fashion and analysed using repeated measures ANOVA. Using a similar method Bartlett and colleagues found that there was relative preservation of right striatal shape in a group that underwent multidisciplinary rehabilitation (Bartlett et al., 2020). Again, correlation with CAG repeats was not done. There is burgeoning evidence that the volume and shape of the striatum in HD may be a suitable structural basis for a biomarker, and the subsequent development of an endophenotype.

1.3. A method to measure spatiotemporal progression

To address the limitations of the current literature (and those of longitudinal shape analysis more broadly, including statistical testing of unbalanced data), we used the Spherical Harmonic Point Distribution Method (SPHARM-PDM) (Styner et al., 2006) to generate point distribution models of shapes for individuals, and used linear mixed models to test for localised shape change over time. We sought to conduct shape analysis using SPHARM-PDM to determine if longitudinal changes in striatal morphology are measurable using different methodology and consistent across methods. As such, we hypothesised that we would find similar results to those seen in pathological studies and in the preliminary longitudinal imaging studies, but that the changes would be resolved in greater detail. Further characterisation of changes during different stages of HD might increase knowledge of neurodegenerative pathways, and progress development of biological measures that may yield single or composite biomarkers for prognostication and use in HD treatment trials. Furthermore, understanding the relationship between quantitative measures of morphology (morphometry) and function *in vivo* may lead to the development of endophenotypes.

2. Methods

2.1. Subjects and measures

As part of the IMAGE-HD project (Georgiou-Karistianis et al., 2013), T1-weighted brain MRI scans were obtained from 36 individuals with pre-HD, 37 with early symp-HD, and 36 healthy matched controls. These scans were repeated 18 months after the initial scan and again 12 months afterwards. 6 controls, 3 pre-HD, and 4 symp-HD subjects were lost to follow up at the second time point, and a further 4 controls, 3 pre-HD, and 4 symp-HD were lost at the third time point. In total, 26 controls, 30 pre-HD, and 29 symp-HD subjects completed all three scans. Healthy controls were matched for age, sex and IQ to the pre-HD individuals. All participants were right-handed.

The IMAGE-HD study was approved by the Monash University and Melbourne Health Human Research Ethics Committees and informed written consent was obtained from each participant prior to testing in accord with the Helsinki Declaration. All testing was undertaken at the Royal Children's Hospital, Parkville, Melbourne, Australia. Ethics approval for this neuroimaging sub-project has also been obtained from both Monash University and from the Australian National University.

Imaging was performed on a Siemens Magnetom Trio Tim System 3 Tesla scanner with a 32-channel head coil (Siemens AG, Erlangen, Germany) at the Murdoch Children's Research Institute (Royal Children's Hospital, Victoria, Australia). High-resolution T1-weighted images were acquired (192 slices, slice thickness of 0.9 mm, 0.8 mm 0.8

mm in-plane resolution 320 × 320 field of view, TI = 900 ms, TE = 2.59 ms, TR = 1900 ms, flip angle = 9°). ICV was calculated from outputs from FMRIB's Software Library FSL 4.1.6 1, for more details see (Georgiou-Karistianis et al., 2013).

2.2. Shape analysis

A single trained researcher (FW) manually segmented the striatum on MRI scans of subjects using a validated protocol (intra-rater intra-class correlation 0.88-0.98) (Looi et al., 2009; 2008) and ANALYZE 11.0 (Mayo Foundation, Rochester, MI, USA) software.

Traced structures were processed for shape analysis using the SPHARM-PDM analysis software (https://www.nitrc.org/projects/spharm-pdm/) (Styner et al., 2006). Segmented 3D binaries were smoothed with a 1mm Gaussian kernel and spherical harmonics were used to generate 1002 corresponding surface points (Levitt et al., 2009; Styner et al., 2006). An average shape was created using the control participants at the baseline time, and all structures were aligned to this mean shape using Procrustes alignment. All shape parametrisations and registrations were manually checked for accuracy. For each participant at each time point, we calculated the signed magnitude of displacement along the surface normal from the mean shape. This displacement vector was used in subsequent shape analysis.

Displacement vector values were used as the dependent variables in all analyses, and all analyses were conducted across the 1002 corresponding points for each structure. We utilised linear mixed models to account for unbalanced longitudinal data with random intercepts and random slopes, addressing repeated time effects (Jakabek et al., 2022). All analyses were performed in R 3.6.2 (R_Core_Team, 2013). For all analyses, estimated total intracranial volume, sex, and baseline age were considered fixed covariates, and time (baseline, 18- and 30 month follow-ups) a fixed factor. Predominant interest was in group and time differences for: (a) between group comparisons, we examined effects of ordinal group, time, and the interaction; and (b) covariate analyses (CAG repeats), we were interested in the group by covariate interaction, time by covariate interaction, and three-way group, time and covariate interaction. For significant group effects we examined post-hoc comparisons between groups using tukey corrections for multiple comparisons. Additionally, *p*-values across each shape were corrected using a False Discovery Rate (FDR) with $p < 0.05$ (Benjamini and Hochberg, 1995). For the purposes of results and discussion, significant differences were only considered at the FDR corrected level.

3. Results

Demographic data as well as striatal volumes can be seen in Table 1. Striatal volumes have been reported in prior papers from the IMAGE-HD consortium and we focus on the shape analyses below.

3.1. Group effects- shape

There was a significant main effect for group type, controlling for different time points (Fig. 1). Widespread deflation was observed over the surface of all structures, with a small amount of inflation in the inferomedial caudate body. Post-hoc analyses showed significant differences between groups in almost all regions of the caudate and putamen, with significant shape deflation in pre-HD compared to controls, and in symp-HD compared to both controls and to pre-HD (Supplementary Figure 1.1 and 1.2).

A significant group by time interaction was observed for the putamen bilaterally (Fig. 2), but not for the caudate, indicating that there was a differential rate of shape change between groups (controls, pre-HD and symp-HD) over time in the putamen only. Participant mean displacement trajectories are included in Supplementary Figure 2. Shape deflation was observed across the anterior and posterior lateral aspects of the right putamen, middle of the lateral aspect of the left putamen, and medial aspects of the putamen bilaterally. Examination of regression slopes indicates that such deflation was more pronounced in the symp-HD group. Post-hoc analyses revealed significant differences in the right putamen, with more rapid deflation over time in symp-HD compared to controls (Supplementary Figure 3).

Table 1
Demographic and volume data across groups.

	Mean ± SD		
	Controls	Pre-HD	Symp-HD
N (Time 1)	36	36	37
N (Time 2)	30	33	33
N (Time 3)	26	30	29
Age at start of study	42 ± 13	42 ± 10	52 ± 9
Sex (M:F)	12:24	14:22	21:16
CAG repeats		42 ± 2	43 ± 2
Estimated YtO		16 ± 7	
Duration of illness (years)			2 ± 2
Total ICV (cm^3)	1457 ± 144	1415 ± 157	1401 ± 156
Baseline bilateral caudate volume (cm^3)	7.4 ± 1.1	6.1 ± 1.6	4.4 ± 1.0
Baseline bilateral putamen volume (cm^3)	6.0 ± 0.8	5.1 ± 1.1	3.4 ± 0.8

CAG repeats, repeat length for trinucleotide expansion coding for polyglutamine repeat in HD; SD, standard deviation; ICV, intracranial volume; YtO, estimated years to disease onset. The ratio of M:F at Time 1 in each group was the same as in Time 3, and mean CAG repeats in pre-HD and symp-HD also remained the same.

3.2. CAG repeats- shape

The main effect of CAG repeats on shape in the HD group (across all groups and time points) occurred for the entire bilateral striatum (Fig. 3). For the putamen, it was across most of the surface, whilst for the caudate, deflation was more prominent in the head and tail, with shape in the medial body largely unrelated to CAG expansion. This association did not differ between groups (pre-HD and symp-HD), i.e., there was no significant group-by-CAG-repeat interaction effect.

In contrast to the lack of group-by-CAG-repeat interaction effect, there was a significant time-by-CAG-repeat interaction effect (Fig. 4). Later time points demonstrated an association between increased CAG repeats and increased deflation in the left caudate head and tail, and right caudate medial body. There were no statistically significant differences between pre-HD and symp-HD in relation to time-by-CAG-repeat effect.

4. Discussion

Using shape analysis combined with linear mixed methods statistical testing (Jakabek et al., 2022), we have been able to visualise and quantify longitudinal shape change in the striatum in HD, specifically with group by time associated with CAG repeat-length. Like prior research we found maximal deflation in the anterior and posterior striatum, which validates our methodology (Muralidharan et al., 2014; Muralidharan et al., 2016; Hong et al., 2017). Additionally, we overcame previous analytical limitations to show accelerated atrophy (i.e., a time interaction effect) of the lateral aspects of the putamen bilaterally, with significantly more rapid shape deflation in the right putamen in symp-HD compared to controls. Interestingly, there was relative preservation of right putamen shape in an interventional study of multidisciplinary rehabilitation in HD, including exercise, perhaps indicating that putamen atrophy may be a marker of motoric dysfunction (Bartlett et al., 2020). Finally, although there is widespread striatal atrophy associated with higher CAG repeats, this is both maximal and shows

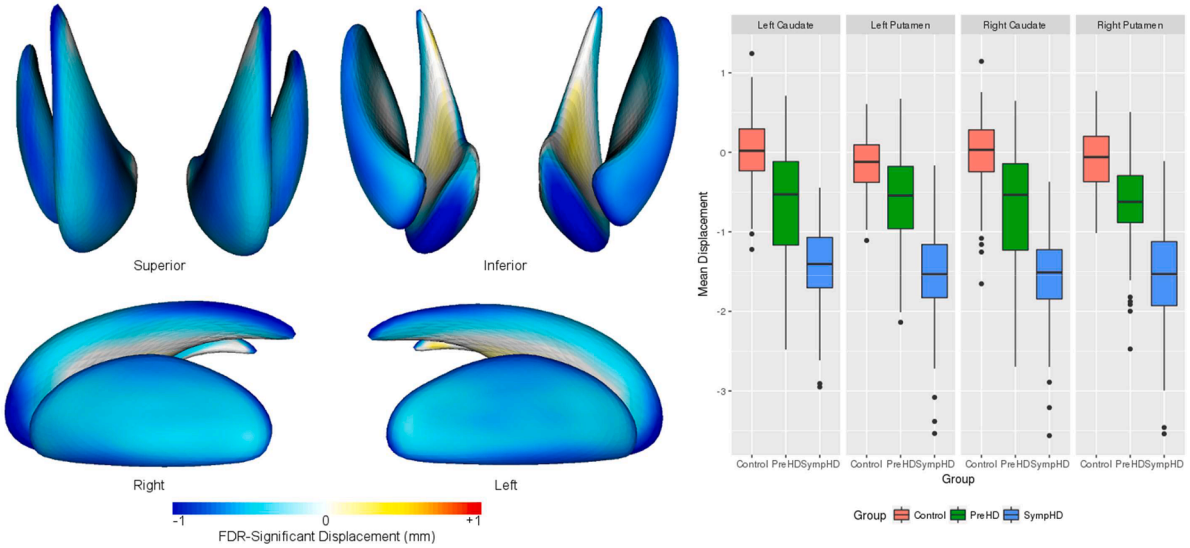

Fig. 1. Main effect of group type, controlling for different time points. Left panels display regions of FDR-significant shape change (in mm) of structures within the striatum from different views. Superior view is in neurological convention, such that left-hand structures are to the left of the view. Inferior view is in radiological convention, such that left-hand images are on the right of the view. Cooler colours indicate shape deflation, warmer colours indicate inflation, and white indicates no significant shape change. The graph on the right plots the mean shape change for significant regions for each participant across groups and structures.

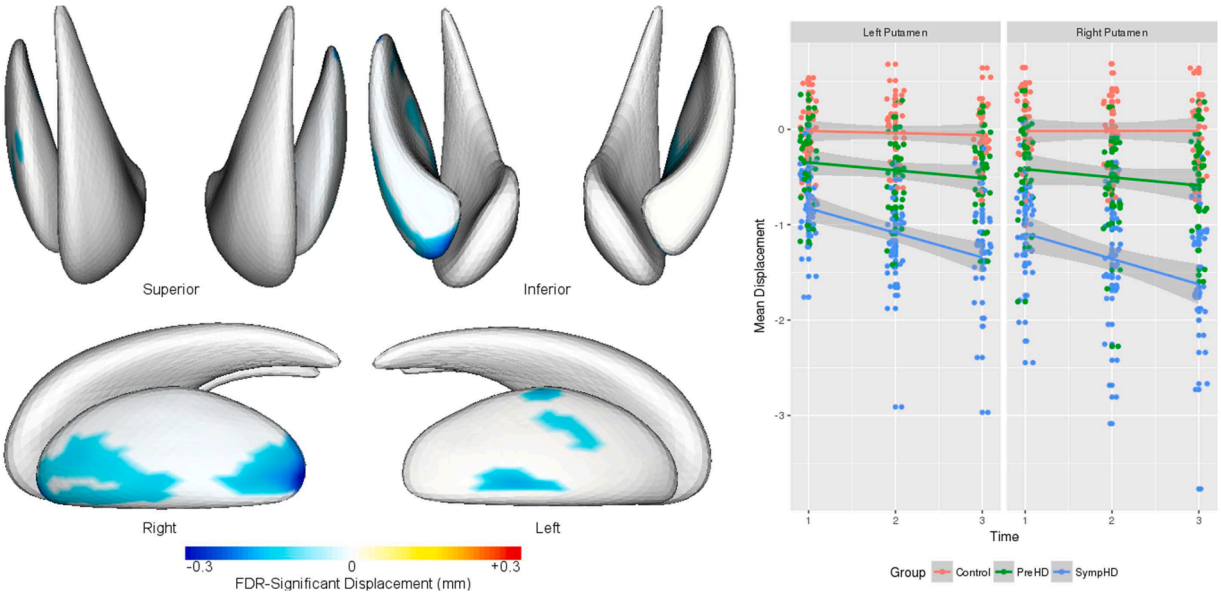

Fig. 2. Group by time interaction. Left panels display regions of FDR-significant shape change (in mm) of structures within the striatum from different views. Superior view is in neurological convention, such that left-hand structures are to the left of the view. Inferior view is in radiological convention, such that left-hand images are on the right of the view. Cooler colours indicate shape deflation, warmer colours indicate inflation, and white indicates no significant shape change. The graph on the right plots the mean shape displacement for significant regions for each participant across time, groups and structures. Shaded areas represent 95% confidence intervals.

accelerated atrophy in the anterior and posterior ends of the striatum. This CAG repeat association finding is novel and extends the findings of previous longitudinal HD shape studies (Muralidharan et al., 2014; Muralidharan et al., 2016; Wijeratne et al., 2018).

4.1. Shape changes in relationship to frontostriatal circuits

Group by time interactions indicating shape deflation in the bilateral putamen implicate a variety of frontostriatal circuits, including motor circuitry as well as re-entrant circuits involving orbitofrontal and dorsolateral prefrontal cortex (impulse control and executive function respectively) (Draganski et al., 2008; Poudel et al., 2019; Tan et al., 2022a; Tan et al., 2022b), and fit with the known deterioration in motor, cognitive, and psychiatric symptoms as HD progresses (Ross and Tabrizi, 2011). Changes in the integrity of these tracts are also seen in cross-sectional studies of pre-HD and symp-HD (Bohanna et al., 2011; Hong et al., 2018; Marrakchi-Kacem et al., 2013; Kloppel et al., 2008), although importantly there is some ability to compensate for deficits at early stages (Kloppel et al., 2009; Turner et al., 2016).

4.2. Implications for pathophysiology

While CAG repeat length plays a dominant role in HD phenotype and contributes approximately 56% of the variation in age of onset of disease

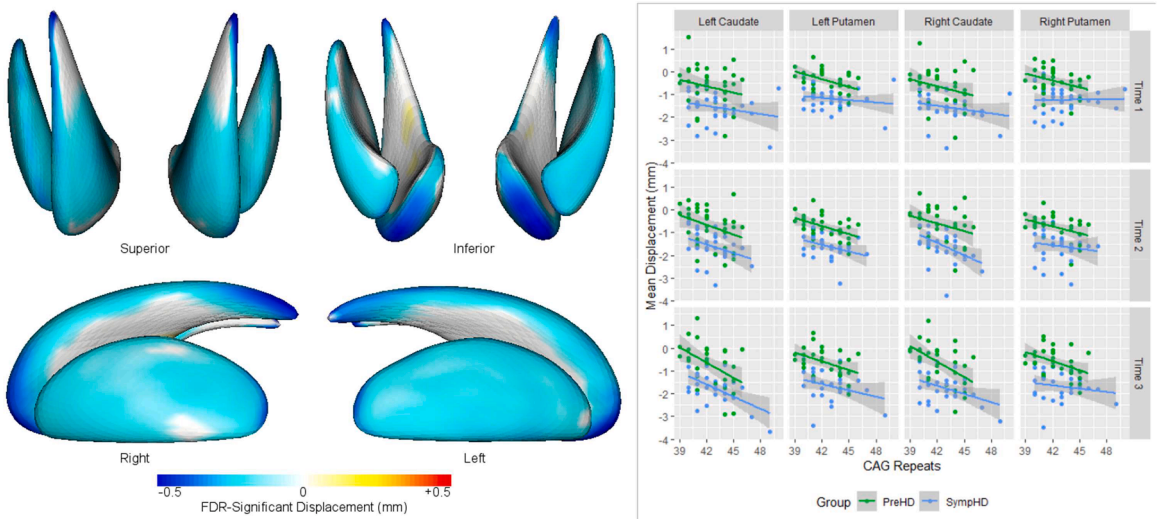

Fig. 3. Main effect of CAG repeats on shape across all groups and time points. Left panels display regions of FDR-significant shape change (in mm) of structures within the striatum from different views. Superior view is in neurological convention, such that left-hand structures are to the left of the view. Inferior view is in radiological convention, such that left-hand images are on the right of the view. Cooler colours indicate shape deflation, warmer colours indicate inflation, and white indicates no significant shape change. The graph on the right plots the association between mean shape displacement and CAG repeats for significant regions for each participant across structures, groups and time.

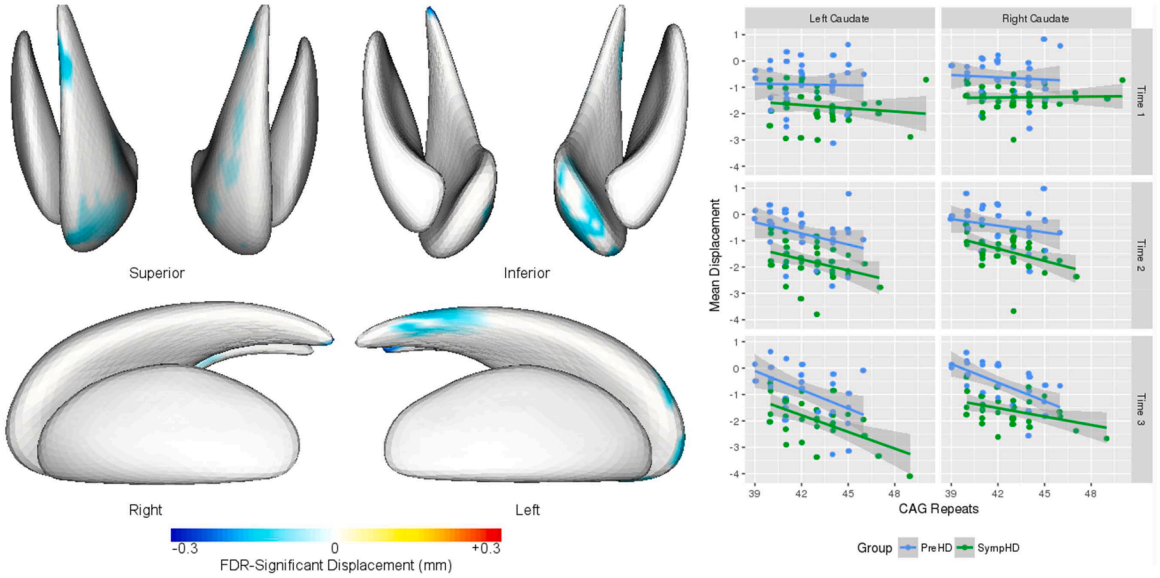

Fig. 4. Time by CAG interaction effect. Left panels display regions of FDR-significant shape change (in mm) of structures within the striatum from different views. Superior view is in neurological convention, such that left-hand structures are to the left of the view. Inferior view is in radiological convention, such that left-hand images are on the right of the view. Cooler colours indicate shape deflation, warmer colours indicate inflation, and white indicates no significant shape change. The graph on the right plots the mean shape change for significant regions for each participant across groups and structures.

(Gusella et al., 2014), other genetic and environmental factors are also thought to play a role (Wexler et al., 2004) although there is less consensus of the role of CAG repeat number in disease progression (Sun et al., 2017; Aylward et al., 2011; Hobbs et al., 2010; Ruocco et al., 2008; Rosas et al., 2011; Langbehn et al., 2019). For striatal volume, longitudinal studies have found an association between CAG repeat number and higher atrophy rates in some brain structures but not necessarily the striatum (Hobbs et al., 2010; Ruocco et al., 2008; Rosas et al., 2011), whereas cross-sectional studies do show an association between CAG repeat number and striatal volume (Aylward et al., 2011; Rosas et al., 2011). More recently, Langbehn and colleagues (Langbehn et al., 2019) have shown early changes in basal ganglia volume which are related to CAG repeat lengths, with linear decreases in volume over time and minimal acceleration with ageing. This contrasts with overall white matter and ventricular changes in the same study which are related to CAG repeat length and continue to accelerate with ageing, and with other overall grey matter volumes which show a far weaker dependence on CAG repeat length and accelerate slightly with age (Langbehn et al., 2019). (Abeyasinghe et al., 2021) using multivariate linear mixed modelling of clinical and volumetric markers in HD, found that individual and combined caudate and putamen volumes differentiated CAG repeat, age groups and progression of disease. These previous studies concur with our novel finding of a CAG-by-time interaction effect for the shape of the caudate being limited to only the very anterior and posterior caudate regardless of group status (pre-HD or symp-HD). Previous research is also consistent with our finding of a group-by-time

interaction involving only the putamen; that is, change in putamen shape over time in symp-HD appears to be somewhat independent of CAG repeat length.

4.3. Towards an endophenotype of HD

Increased shape deflation in the putamen with time is consistent with some previous volumetric work (Tabrizi et al., 2009; Wijeratne et al., 2018), although of note a recent analysis combining brain volumes from the PREDICT-HD, TRACK-HD and IMAGE-HD studies showed that caudate volume was the best (volumetric) imaging marker for pre-HD (Wijeratne et al., 2020). However, using caudate volume as a biomarker for potential treatment trials would still require 661 participants in a study to achieve power of >80% assuming a 20% treatment effect. This study pooled data from three studies, with significant differences amongst groups and total motor score, which may explain some of the differences in results. They also found that effect sizes for volume changed varied with disease burden score of the people in the individual studies (Wijeratne et al., 2020). Shape was not investigated in that study and may provide more subtle anatomical detail which is missed by broader volumetric studies, potentially providing a better opportunity to test prospective treatments. Our sample is small and has a relatively low disease burden score in pre-HD compared to others (Wijeratne et al., 2020), and further replication is needed to confidently assert that shape may be superior to volume. However our initial findings are encouraging. The complexity of changes in HD, found in our study and increasingly highlighted in the literature, indicate the usefulness of composite structural morphological measures, including shape analysis, to construct an endophenotype of HD.

4.4. Limitations

Despite this advantage over previous work, a limitation of the current methodology is the identification of shape change only along the surface normal. Thus, significant stretching or shearing is not captured, reducing the sensitivity of the analysis. Shape effects are relatively small (in the order of several millimetres) and may be confounded by partial volume effects in image acquisition and subsequent tracing, shape parameterisation, and shape registration. This study also used manual tracing of the putamen and caudate over three time periods as the basis for longitudinal shape analysis. This labour-intensive method is limited by the need to have an experienced tracer and the increased amount of time necessary for manual tracing. Nonetheless, we believe that manual tracing is currently superior to automated methods of segmentation (Looi et al., 2009; 2008).

Some medial caudate inflation (indicated by warmer colours) was seen in this study, related to group type (Fig. 1) and CAG repeat number (Fig. 3). This may be an artefact related to two different processes. Firstly, there is ventricular expansion and consequent relative flattening of the caudate nucleus with progression of HD. Secondarily, shape change here is measured relative to the vertex normal (i.e., perpendicular to the surface) which is less well able to capture more complex shape deformations such as bending and shearing. However, it has the benefit of being able to be integrated in mixed models for longitudinal analysis. Overall, we suspect that there is both complex shape change and atrophy, the latter of which is indicated by a larger magnitude of shape deflation than inflation.

It is important to also note that the shape changes seen here occur over a relatively small snapshot of time (2.5 years), in people who are either still many years from predicted diagnosis of HD or who have only recently been diagnosed with HD. This may be responsible for the fact that significant longitudinal shape change was only seen in symp-HD in the putamen and not the caudate, and no longitudinal change was seen in pre-HD, despite the fact that there are baseline differences in both. The relatively small sample size here may also limit interpretation.

4.5. Conclusions/clinical implications

We have mapped longitudinal shape change in the striatum in HD, confirming the findings of previous linear mixed model shape analysis and parallel shape analysis methodologies. We have demonstrated that robust statistical analysis of shape change in HD is practicable. Such shape analysis linear mixed model methods have important implications for the development of a morphological biomarker in HD. These methods allow spatiotemporal signatures to be derived for the progression of atrophy of the striatum in HD. These spatiotemporal signatures may assist in understanding pathophysiology towards prognostication and analysing the effectiveness of disease-modifying treatments. Further characterisation of these changes increases knowledge of neurodegenerative pathways and the relationship between striatal shape and function *in vivo*, constituting an endophenotype, and a potential biomarker for prognostication and use in HD treatment trials.

CRediT authorship contribution statement

F.A. Wilkes was involved in conceptualisation, data curation, formal analysis, investigation and methodology of this imaging sub-project of the IMAGE-HD project. She also wrote the original draft and orchestrated the review and editing of the final manuscript. D. Jakabek developed and performed the longitudinal statistical shape analysis. He was central to formal analysis, investigation and methodology of this subproject, as well as being involved in the review and editing of the final manuscript. G. Poudel, J.C. Stout, P. Chua, and G.F. Egan were involved in conceptualisation, data curation, formal analysis, funding acquisition, investigation, methodology, and project administration of the main IMAGE-HD project, from which this article draws its data. They were also all involved in the review and editing of the final version of this manuscript. N. Georgiou-Karistianis is the primary investigator of the IMAGE-HD project and so was integral to all of the above roles related to the IMAGE-HD main project, as well as visualisation of the main project and this sub-project, review and editing of the manuscript, and supervision of F.A. Wilkes as her PhD co-supervisor. M. Walterfang and D. Velakoulis were involved in conceptualisation of this sub-project, as well as supervision of F.A. Wilkes as her PhD co-supervisors. They were also involved in the review and editing of the final manuscript. J.C. L. Looi was involved in conceptualisation of this sub-project, supervision of F.A. Wilkes as her main PhD supervisor, and review and editing of the final manuscript. All authors had significant intellectual and practical input into the final manuscript.

Declaration of Competing Interest

J.C. Stout has received funding from CHDI Foundation unrelated to this research. She is also director of Zindametrix Pty Ltd., which has research contracts supporting the implementation of cognitive assessments in HD clinical trials, none of which are relevant to this research. J. C.L. Looi self-funded travel and computer infrastructure costs to coordinate this research through the Australian United States Scandinavian-Spanish Imaging Exchange (AUSSIE), based at the Australian National University Medical School. M. Walterfang has received funding for research from and has received honoraria from Actelion, Vtesse and Biomarin pharmaceuticals, unrelated to this research.

Funding sources for study

This work was supported by the CHDI Foundation, Inc. (USA) (grant number A –3433); the National Health and Medical Research Council (NHMRC) (grant number 606650); the RANZCP New Investigator Grant 2013 (FAW); and the University of Melbourne – computer and software support. We thank all participants for their involvement in the study.

Supplementary materials

Supplementary material associated with this article can be found, in the online version, at doi:10.1016/j.pscychresns.2023.111717.

References

Abeyasinghe, PM, Long, JD, Razi, A, et al., 2021. Tracking Huntington's disease progression using motor, functional, cognitive, and imaging markers. Move. Disord. 36, 2282–2292.

Aylward, EH, Nopoulos, PC, Ross, CA, et al., 2011. Longitudinal change in regional brain volumes in prodromal Huntington disease. J. Neurol. Neurosurg. Psychiatry 82, 405–410.

Bartlett, DM, Govus, A, Rankin, T, et al., 2020. The effects of multidisciplinary rehabilitation on neuroimaging, biological, cognitive and motor outcomes in individuals with premanifest Huntington's disease. J. Neurol. Sci. 416, 117022.

Benjamini, Y, Hochberg, Y., 1995. Controlling the false discovery rate—a practical and powerful approach to multiple testing. J. R. Stat. Soc. B Met. 57, 289–300.

Bohanna, I, Georgiou-Karistianis, N, Egan, GF., 2011. Connectivity-based segmentation of the striatum in Huntington's disease: vulnerability of motor pathways. Neurobiol. Dis. 42, 475–481.

Cruickshank, T, Reyes, A, Pulverenti, TS, et al., 2020. Rate of torque development and striatal shape in individuals with prodromal Huntington's disease. Scient. Rep. 10, 15103.

Douaud, G, Gaura, V, Ribeiro, MJ, et al., 2006. Distribution of grey matter atrophy in Huntington's disease patients: A combined ROI-based and voxel-based morphometric study. Neuroimage 32, 1562–1575.

Draganski, B, Kherif, F, Kloeppel, S, et al., 2008. Evidence for segregated and integrative connectivity patterns in the human basal ganglia. J. Neurosci. 28, 7143–7152.

Georgiou-Karistianis, N, Gray, MA, Dominguez, JF, et al., 2013. Automated differentiation of pre-diagnosis Huntington's disease from healthy control individuals based on quadratic discriminant analysis of the basal ganglia: The IMAGE-HD study. Neurobiol. Dis. 51, 82–92.

Gottesman, II, Gould, TD, 2003. The endophenotype concept in psychiatry: etymology and strategic intentions. Am. J. Psychiatry 160, 636–645.

Gusella, JF, MacDonald, ME, Lee, JM, 2014. Genetic modifiers of Huntington's disease. Mov. Disord. 29, 1359–1365.

Hobbs, NZ, Barnes, J, Frost, C, et al., 2010. Onset and progression of pathologic atrophy in Huntington disease: a longitudinal MR imaging study. AJNR Am. J. Neuroradiol. 31, 1036–1041.

Hong, S, Fishbaugh, J, Rezanejad, M, et al., 2017. Subject-specific longitudinal shape analysis by coupling spatiotemporal shape modeling with medial analysis. Proc. SPIE Int. Soc. Opt. Eng. 10133.

Hong, Y, O'Donnell, LJ, Savadjiev, P, et al., 2018. Genetic load determines atrophy in hand cortico-striatal pathways in presymptomatic Huntington's disease. Hum. Brain Mapp. 39, 3871–3883.

Jakabek, D, Rae, CD, Brew, BJ, et al., 2022. Brain aging and cardiovascular factors in HIV: a longitudinal volume and shape MRI study. AIDS 36, 785–794.

Kassubek, J, Juengling, FD, Kioschies, T, et al., 2004. Topography of cerebral atrophy in early Huntington's disease: a voxel based morphometric MRI study. J. Neurol. Neurosurg. Psychiatry 75, 213–220.

Kloppel, S, Draganski, B, Golding, CV, et al., 2008. White matter connections reflect changes in voluntary-guided saccades in pre-symptomatic Huntington's disease. Brain 131, 196–204.

Kloppel, S, Draganski, B, Siebner, HR, et al., 2009. Functional compensation of motor function in pre-symptomatic Huntington's disease. Brain 132, 1624–1632.

Langbehn, DR, Stout, JC, Gregory, S, et al., 2019. Association of CAG Repeats With Long-term Progression in Huntington Disease. JAMA Neurol.

Levitt, JJ, Styner, M, Niethammer, M, et al., 2009. Shape abnormalities of caudate nucleus in schizotypal personality disorder. Schizophrenia Res. 110, 127–139.

Looi, JCL, Lindberg, O, Liberg, B, et al., 2008. Volumetrics of the caudate nucleus: Reliability and validity of a new manual tracing protocol. Psychiatry Res. Neuroimag. 163, 279–288.

Looi, JCL, Rajagopalan, P, Walterfang, M, et al., 2012. Differential putaminal morphology in Huntington's disease, frontotemporal dementia and Alzheimer's disease. Aust. N.Z. J. Psychiatry.

Looi, JCL, Santillo, AF, 2017. Time and relative dimensions in syndromology: Towards endophenotypes in neurology, psychiatry and in-between. Aust. N. Z. J. Psychiatry 51, 1079–1081.

Looi, JCL, Svensson, L, Lindberg, O, et al., 2009. Putaminal volume in frontotemporal lobar degeneration and Alzheimer disease: differential volumes in dementia subtypes and controls. Am. J. Neuroradiol. 30, 1552–1560.

Looi, JCL, Walterfang, M, 2012. Striatal morphology as a biomarker in neurodegenerative disease. Mol. Psychiatry 18, 417–424.

Marrakchi-Kacem, L, Delmaire, C, Guevara, P, et al., 2013. Mapping cortico-striatal connectivity onto the cortical surface: a new tractography-based approach to study Huntington disease. Plos One 8, e53135.

Muralidharan, P, Fishbaugh, J, Johnson, HJ, et al., 2014. Diffeomorphic shape trajectories for improved longitudinal segmentation and statistics. Med. Image Comput. Comput. Assist. Interv. 17, 49–56.

Muralidharan, P, Fishbaugh, J, Kim, EY, et al., 2016. Bayesian covariate selection in mixed-effects models for longitudinal shape analysis. Proc. IEEE Int. Symp. Biomed. Imaging 0, 656–659.

Poudel, GR, Harding, IH, Egan, GF, et al., 2019. Network spread determines severity of degeneration and disconnection in Huntington's disease. Hum. Brain Mapp. 40, 4192–4201.

R_Core_Team, 2013. R: a language and environment for statistical computing. R Foundation for Statistical Computing, Vienna, Austria.

Ramirez-Garcia, G, Galvez, V, Diaz, R, et al., 2020. Longitudinal atrophy characterization of cortical and subcortical gray matter in Huntington's disease patients. Eur. J. Neurosci. 51, 1827–1843.

Roos, R, Pruyt, J, de Vries, J, et al., 1985. Neuronal distribution in the putamen in Huntington's disease. J. Neurol. Neurosurg. Psychiatry 48, 422–425.

Rosas, HD, Reuter, M, Doros, G, et al., 2011. A tale of two factors: what determines the rate of progression in Huntington's Disease? A longitudinal MRI study. Move. Disord. 26, 1691–1697.

Ross, CA, Tabrizi, SJ, 2011. Huntington's disease: from molecular pathogenesis to clinical treatment. Lancet Neurol. 10, 83–98.

Ruocco, HH, Bonilha, L, Li, LM, et al., 2008. Longitudinal analysis of regional grey matter loss in Huntington disease: effects of the length of the expanded CAG repeat. J. Neurol. Neurosurg. Psychiatry 79, 130–135.

Styner, M, Oguz, I, Xu, S, et al., 2006. Framework for the statistical shape analysis of brain structures using SPHARM-PDM. Insight J. 1071, 242–250.

Sun, YM, Zhang, YB, Wu, ZY., 2017. Huntington's disease: relationship between phenotype and genotype. Mol. Neurobiol. 54, 342–348.

Tabrizi, SJ, Langbehn, DR, Leavitt, BR, et al., 2009. Biological and clinical manifestations of Huntington's disease in the longitudinal TRACK-HD study: cross-sectional analysis of baseline data. Lancet Neurol. 8, 791–801.

Tan, B, Shishegar, R, Fornito, A, et al., 2022a. Longitudinal mapping of cortical surface changes in Huntington's Disease. Brain Imag. Behav. 16, 1381–1391.

Tan, B, Shishegar, R, Oldham, S, et al., 2022b. Investigating longitudinal changes to frontal cortico-striatal tracts in Huntington's disease: the IMAGE-HD study. Brain Imag. Behav.

Turner, LM, Jakabek, D, Wilkes, FA, et al., 2016. Striatal morphology correlates with frontostriatal electrophysiological motor processing in Huntington's disease: an IMAGE-HD study. Brain Behav. 6, e00511.

van den Bogaard, SJA, Dumas, EM, Acharya, TP, et al., 2011a. Early atrophy of pallidum and accumbens nucleus in Huntington's disease. J. Neurol. 258, 412–420.

van den Bogaard, SJA, Dumas, EM, Ferrarini, L, et al., 2011b. Shape analysis of subcortical nuclei in Huntington's disease, global versus local atrophy - Results from the TRACK-HD study. J. Neurol. Sci. 307, 60–68.

Vonsattel, JP, Myers, RH, Stevens, TJ, et al., 1985. Neuropathological classification of Huntington's disease. J. Neuropathol. Exp. Neurol. 44, 559–577.

Vonsattel, JPG, DiFiglia, M, 1998. Huntington disease. J. Neuropathol. Experim. Neurol. 57, 369–384.

Wexler, NS, Lorimer, J, Porter, J, et al., 2004. Venezuelan kindreds reveal that genetic and environmental factors modulate Huntington's disease age of onset. Proc. Natl Acad. Sci. U S A 101, 3498–3503.

Wijeratne, PA, Garbarino, S, Gregory, S, et al., 2021. Revealing the timeline of structural MRI changes in premanifest to manifest Huntington disease. Neurol. Genet. 7, e617.

Wijeratne, PA, Johnson, EB, Eshaghi, A, et al., 2020. Robust markers and sample sizes for multicenter trials of Huntington disease. Ann. Neurol. 87, 751–762.

Wijeratne, PA, Young, AL, Oxtoby, NP, et al., 2018. An image-based model of brain volume biomarker changes in Huntington's disease. Ann. Clin. Transl. Neurol. 5, 570–582.

Younes, L, Ratnanather, T, Brown, T, et al., 2012. Regionally selective atrophy of subcortical structures in prodromal HD as revealed by statistical shape analysis. Hum. Brain Mapp.